MECHANOCHEMISTRY

Mechanochemical unzipping of insulating polyladderene to semiconducting polyacetylene

Zhixing Chen,[1] Jaron A. M. Mercer,[1] Xiaolei Zhu,[1,2,4] Joseph A. H. Romaniuk,[1] Raphael Pfattner,[3] Lynette Cegelski,[1] Todd J. Martinez,[1,2,4]* Noah Z. Burns,[1]* Yan Xia[1]*

Biological systems sense and respond to mechanical stimuli in a complex manner. In an effort to develop synthetic materials that transduce mechanical force into multifold changes in their intrinsic properties, we report on a mechanochemically responsive nonconjugated polymer that converts to a conjugated polymer via an extensive rearrangement of the macromolecular structure in response to force. Our design is based on the facile mechanochemical unzipping of polyladderene, a polymer inspired by a lipid natural product structure and prepared via direct metathesis polymerization. The resultant polyacetylene block copolymers exhibit long conjugation length and uniform trans-configuration and self-assemble into semiconducting nanowires. Calculations support a tandem unzipping mechanism of the ladderene units.

Mechanical force can induce chemical transformations that are inaccessible under traditional thermal or photochemical reaction manifolds (*1*–*3*). Force-based signaling manifests in macromolecules that can transduce strong pulling or shearing forces along their backbone. In biological systems, cellular transduction of mechanical stimuli to electrical signals underlies tactile and auditory sensation, muscle contraction, and many other important physiological processes (*4*). Emergent polymer mechanochemistry has transformed chemists' ability to explore force-induced reactivity: Various molecular motifs, termed mechanophores, have been elaborately designed to undergo productive chemical transformations in response to mechanical stimuli, conferring force-responsive properties to polymers, such as coloration (*5*), luminescence (*6*, *7*), self-strengthening (*8*), and self-demolishing (*9*), as well as release of small molecules (*10*, *11*) and active catalysts (*12*). Most examples to date involve sparse incorporation of a reporter mechanophore into a mechanochemically inert polymer; moving forward, a central challenge is achieving (macro)molecular design to enable mechanochemical transformations of an entire polymer chain, resulting in amplified, synergistic changes to its molecular and macroscopic properties. Herein, we report a macromolecular scaffold that rearranges dramatically under force, converting a series of strained σ bonds to π bonds, thus transforming an insulating nonconjugated structure to a semiconducting structure with continuous extended conjugation.

[1]Department of Chemistry, Stanford University, Stanford, CA 94305, USA. [2]The PULSE Institute, Stanford University, Stanford, CA 94305, USA. [3]Department of Chemical Engineering, Stanford University, Stanford, CA 94305, USA. [4]SLAC National Accelerator Laboratory, Menlo Park, CA 94025, USA.
*Corresponding author. Email: toddmtz@stanford.edu (T.J.M.); nburns@stanford.edu (N.Z.B.); yanx@stanford.edu (Y.X.)

Conjugated polymers possess a range of distinct optical, electronic, thermal, and mechanical properties that are widely applied in sensing, imaging, energy harvesting, and flexible electronics (*13*). The ability to trigger these properties by mechanical stimulation would allow access to smart materials with a suite of output responses and functions upon mechanical input. Such a goal, however, presents two formidable challenges: (i) linking a vast number of mechanophores repeatedly along the force path in a polymer chain and (ii) mechanically triggering the change of sp^3 to sp^2 hybridization state in a continuous stretch of backbone carbons to establish extended conjugation.

Strained four-membered cyclobutane and cyclobutene rings have been explored by Moore, Boulatov, and Craig as mechanophores to generate a pair of olefins under force (*1*, *14*–*18*). We hypothesized that cyclobutenes (CBEs) might bridge separate π motifs with an insulating yet mechanically labile σ bond, allowing mechanical activation to establish continuous conjugation (Fig. 1A). Our initial efforts to synthesize various CBEs with alkenyl or aryl substituents at the 3 and 4 positions (**1**) failed, presumably due to facile thermal electrocyclic ring-opening at room temperature (Fig. 1B) (*19*, *20*). Seeking an alternative strategy, we postulated that fusion of one or more mechanically active cyclobutane rings between the CBE and the destabilizing π linkages could enhance thermal stability (Fig. 1C). Our inspiration came from the intriguing structure of the naturally occurring ladderane lipids (as in fatty acid **5**, Fig. 1D), which make up a large fraction of the membrane lipids produced by anaerobic ammonium oxidizing (anammox) bacteria (*21*). We envisioned that multiple fused cyclobutanes in [*n*]-ladderanes (where *n* refers to the number of fused four-membered rings) could undergo tandem [2+2] cycloreversions via mechanochemical unzipping to generate oligoenes (Fig. 1C). Some of us recently developed a concise total synthesis of [5]-ladderane lipids (*22*). Therefore, we designed our ladderene mechanophore monomer based on [5]-ladderane (Fig. 1E), although ladderenes of any length (any *n*) could be leveraged as mechanophores to generate oligoenes in principle. The next step in the design required connecting repeated ladderene structures efficiently into a polymer: Direct polymerization of mechanophores seemed the simplest and most effective way to synthesize the mechanochemically active polymers. We anticipated that simple ring-opening

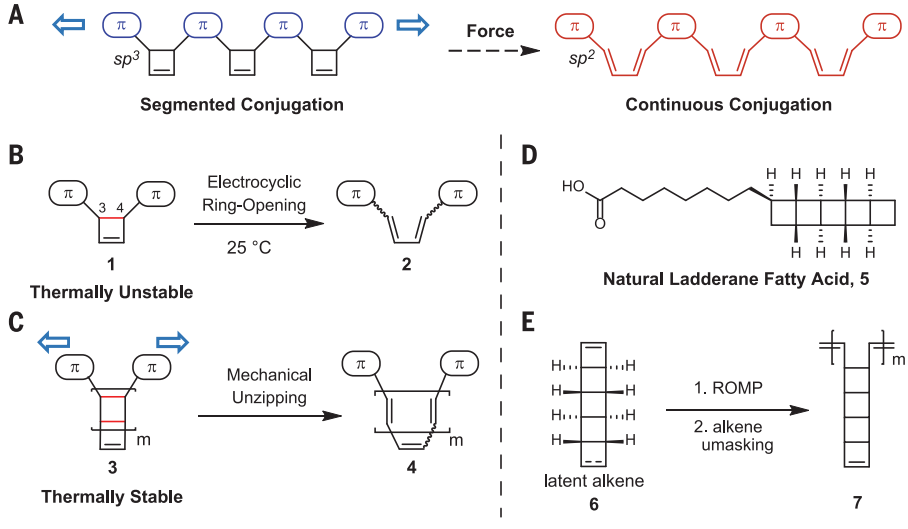

Fig. 1. Design of mechanochemically generated conjugated polymer. (**A**) Insulating CBE mechanophores connected with π systems, designed to rearrange to continuously extended conjugation under force. (**B**) Thermally unstable CBEs with sp^2 carbon substituents at the 3 and 4 positions. (**C**) Ladderene-based mechanophore, which would undergo tandem mechano-cycloreversions to give conjugated oligoene. (**D**) Natural [5]-ladderane fatty acid (**5**) from anammox bacteria. (**E**) Design of mechanically active polyladderene via ROMP of ladderene.

metathesis polymerization (ROMP) (*23*) would be an ideal method to polymerize ladderene, driven by the release of CBE strain, and also conveniently generate the requisite polymer backbone π-bond connection between mechanophores (Fig. 1E). Polyladderenes of this type comprise exclusively methine carbons and would be expected to unzip to polyacetylene (PA) (*24*) upon successful mechanochemical activation.

We designed chloroladderene **10** (Fig. 2A) as the ROMP monomer for the synthesis of polyladderene. Chloroladderene **10** is a latent ladderdiene: One CBE undergoes ROMP to give linear poly(chloroladderane) **11**; subsequently, the second CBE is unmasked at the end of each ladder by elimination of HCl to give polyladderene **7**. We prepared **10** from previously synthesized chloroladderane **8** (*22*) via a second chlorination under Groves' Mn-porphyrin conditions (*25*), followed by elimination of one of the chlorides with KO*t*-Bu. Monomer **10** readily polymerized to nearly full conversion within 1 hour at room temperature in chloroform upon addition of 0.1 to 0.5 mole % (mol %) of fast-initiating Grubbs III catalyst. Gel permeation chromatography (GPC) analysis of the resulting poly(chloroladderane) **11** revealed a narrow molecular weight (MW) distribution with MW proportional to the monomer-to-catalyst ratio, which was varied from 200 to 1000 (Fig. 2B). These features indicated controlled ROMP to be an efficient strategy to produce polymers with hundreds of linked mechanophores. Treatment of the polymer **11** with 1 M KO*t*-Bu in tetrahydrofuran (THF) at 16°C yielded polyladderene **7** with complete elimination of HCl and generation of a terminal CBE on all ladder side chains (Fig. 2C). Polymers **7** showed slower elution in GPC and a decrease in MW compared with their corresponding precursors **11** (**7a**, **7b**, and **7c**: M_n = *93*, *63*, and *34* kDa, respectively). For the very-high-MW polymer (**7a**), broadening of the MW distribution was observed after elimination; however, high-MW polyladderenes were still obtained.

We then studied the mechanochemical activation of polyladderene **7a** in THF solution using controlled ultrasonication, a convenient and standard technique to apply mechanical force in an acoustic flow and thereby study polymer mechanochemistry (Fig. 3A). After only 20 s of sonication, the initially colorless polymer solution turned blue and then continued to darken. After 120 min of sonication, the reaction mixture had turned dark blue/purple, with concomitant formation of black precipitate on the side of the glass vessel (Fig. 3B). Solution aliquots were drawn with a syringe at different time points during sonication and analyzed by ultraviolet-visible (UV-vis) spectroscopy (Fig. 3C). A broad absorption peak with a maximum over 600 nm and an onset at 850 nm were clearly and consistently observed throughout the course of sonication. These observed wavelengths are among the highest reported for solution-synthesized PAs (*26*–*29*), suggesting the formation of PA blocks with long conjugation lengths. The absorption peak continuously grew in intensity during the sonication process, indicating continuous formation of PA. After 120 min of sonication, the absorption maximum slightly shifted hypsochromically to 605 nm with a concomitant decrease in solubility and formation of particulates due to the relatively high content of insoluble PA. Long-wavelength absorption was observed even at the beginning of sonication, when the absorbance was still low (fig. S1). This observation suggests that, even though only a small fraction of the polymer solution was processed at each pulse of sonication, long strands of PA, rather than multiple segments of oligoenes, were rapidly formed within that fraction of sample. To prove the mechanochemical nature of the polyladderene transformation, we subjected polyladderenes of different MWs to identical sonication conditions. The kinetics of the mechanochemical formation of PA strongly depended on the MW of precursor polymer: Polyladderenes with lower MWs formed PA more slowly but with similar optical absorption profiles (fig. S2). Because thermal activation is not affected by the polymer MW, these MW-dependent kinetics are commonly regarded as strong evidence for mechanochemistry.

We applied several spectroscopic and microscopic methods to characterize the structure of mechanochemically generated PA copolymer **12**. Cross-polarization magic-angle spinning ^{13}C solid-state nuclear magnetic resonance (NMR) spectroscopy was used to analyze the isolated activated polymer. A carbon resonance at 136 parts per million corresponding to *trans*-PA was clearly observed (*30*), along with the signals associated with the residual polyladderene (Fig. 3D). Based on the integrations of sp^2 and sp^3 carbon signals, the conversion of polyladderene **7a** to PA was determined to be ~37% after 120 min of sonication (fig. S3).

Resonant Raman spectra (785-nm excitation) of samples after 20 s and 20 min of sonication exhibited vibrational peaks at 1463 and 1073 cm^{-1}, matching the C=C and C–C stretching peaks for *trans*-PA, respectively (Fig. 3E) (*31*). Both the Raman frequency at 1463 cm^{-1} and visible absorption peak at 636 nm suggested the formation of very long *trans*-PA with > 100 conjugated C=C bonds, based on the reported correlations (*32*). Infrared (IR) spectra of the resulting polymer **12** exhibited an intense peak at 1012 cm^{-1}, corresponding to the reported C–H bending of *trans*-PA, as well as peaks at 2924 and 2851 cm^{-1} for the C–H stretches of cyclobutane in the remaining unactivated ladderene (fig. S5). No signals corresponding to cis configuration of PA were observed within the detection limit of IR or ^{13}C NMR experiments (figs. S3 and S5). Because each ladderene side chain bears a *cis*-olefin at the terminus, the absence of *cis*-olefin signals suggests simultaneous mechanochemical cis-to-trans isomerization during the PA generation. These spectroscopic data collectively confirmed the mechanochemical transformation of polyladderene to *trans*-PA with remarkably uniform configuration and long conjugation length.

The force exerted onto a polymer chain via sonication is known to peak near the middle of the chain (*33*). Thus, we expect mechanochemical unzipping to occur from the middle of the chain where the force is above the activation threshold, resulting in the formation of ABA-type triblock

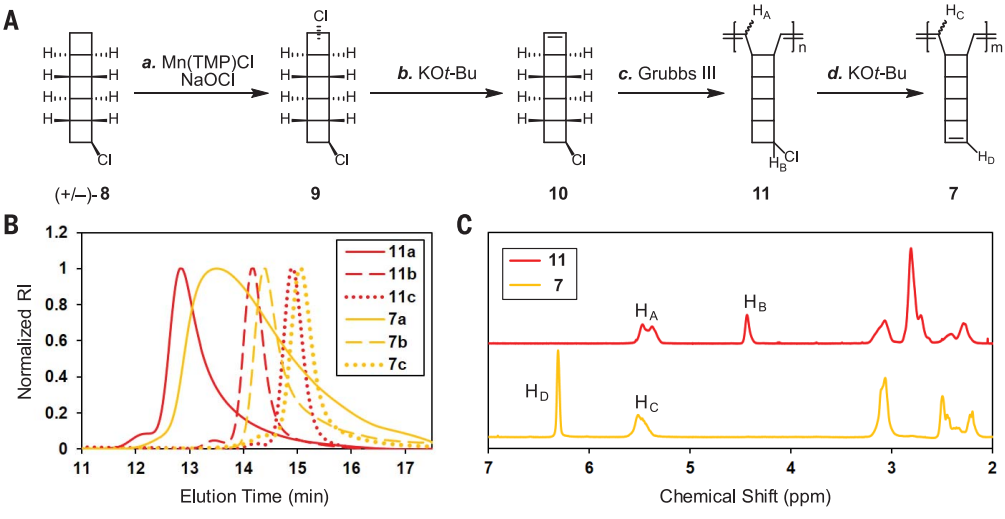

Fig. 2. Synthesis of polyladderene. (**A**) Synthetic route to polyladderene **7**. (a) Mn(III) meso-tetra(2,4,6-trimethylphenyl)porphine chloride (5 mol %), NaOCl (7.2 equiv.), tetra-*n*-butylammonium chloride (12 mol %), CH_2Cl_2/H_2O, 23°C, 4 hours, 37%, 31% recovered starting material (rsm). (b) KO*t*-Bu (1 equiv.), THF, 35°C, 3 hours, 49%, 38% rsm. (c) Grubbs III catalyst (0.1, 0.25, or 0.5 mol %), $CHCl_3$, 25°C, 6 hours, quantitative conversion. (d) KO*t*-Bu (50 equiv.), THF, 16°C, 40 hours, quantitative conversion. (**B**) GPC traces of polymers **11**, **a** to **c**, and **7**, **a** to **c**. (**C**) ^1H NMR spectra of polymers **11** and **7**.

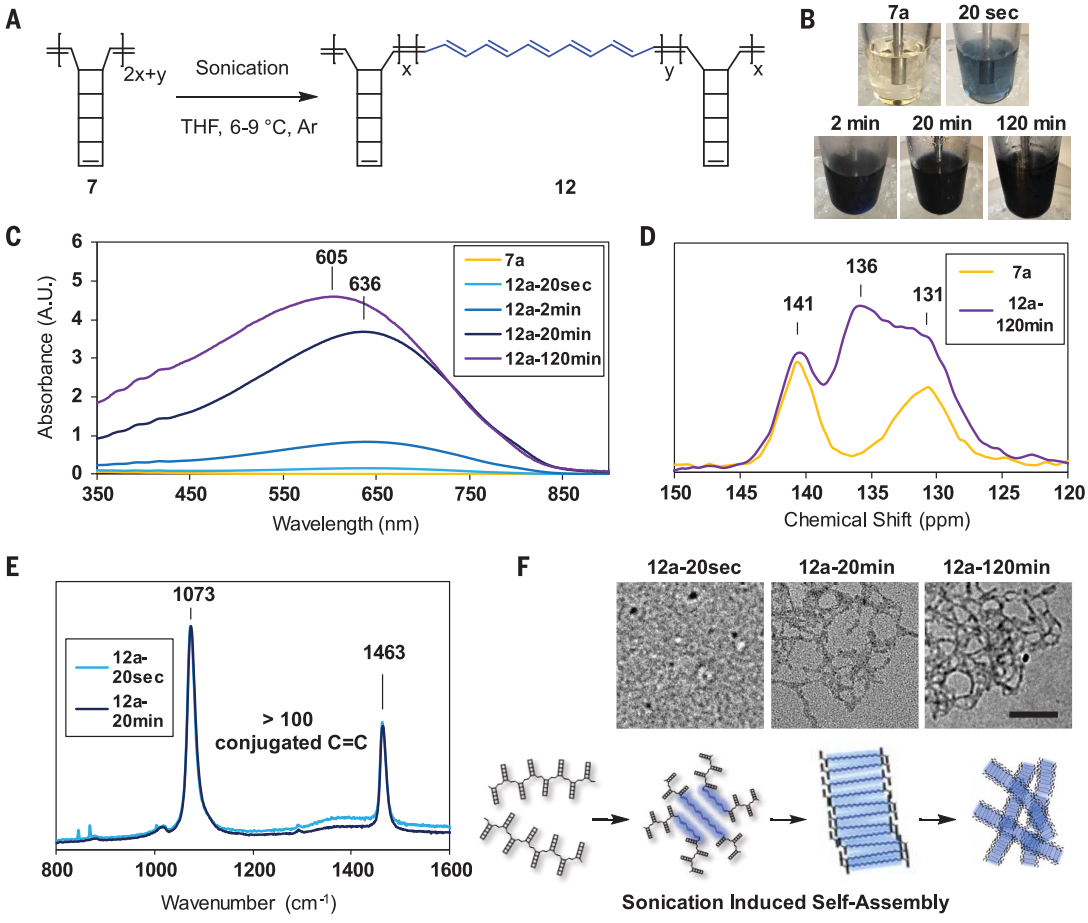

Fig. 3. Characterization of the mechanochemically generated PA copolymer from polyladderene. (**A**) Reaction scheme for mechanochemical conversion of polyladderene **7** to PA-containing block copolymer **12**. (**B**) Photographs of reaction vessel at different sonication times. (**C**) UV-vis absorption spectra of sonicated **7a** solution at different sonication times. (**D**) Overlaid solid-state ^{13}C NMR spectra of polymers **7a** and **12a** after 120 min of sonication. (**E**) Resonance Raman spectra of the sonication products (785-nm laser excitation). (**F**) TEM images of the nanostructures formed during sonication (scale bar, 200 nm) and proposed sonication-induced self-assembly of the resultant block copolymer.

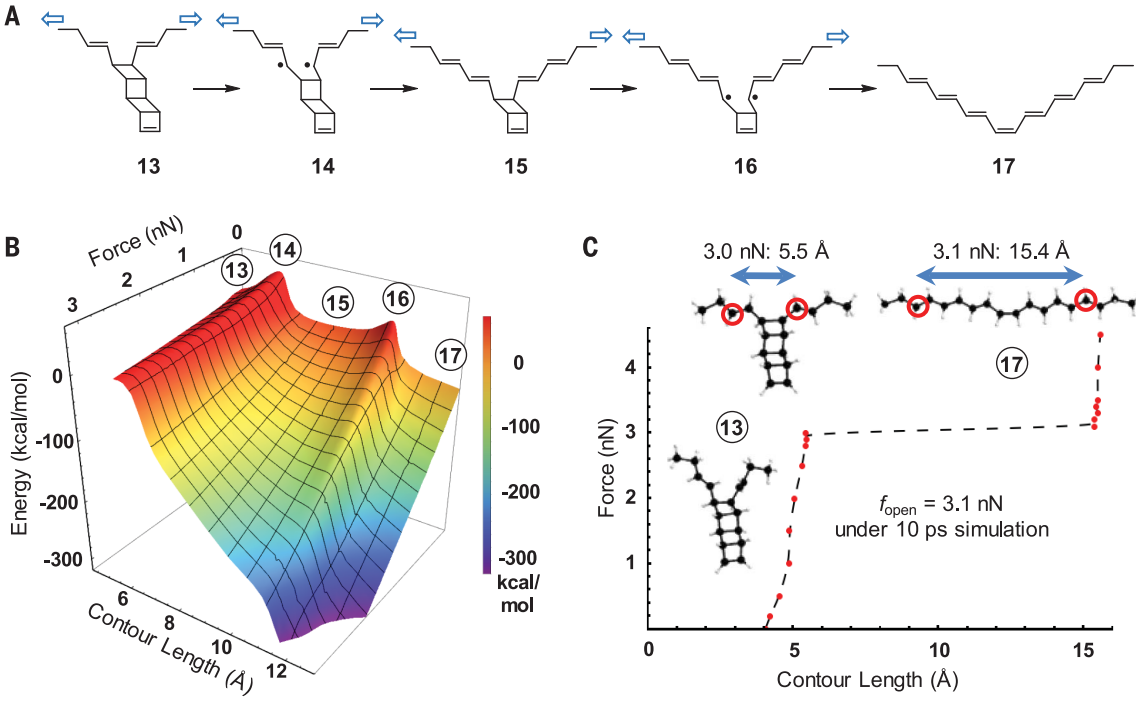

Fig. 4. Theoretical simulation of the unzipping process of a ladderene unit. (**A**) Proposed reaction pathway for mechanochemical unzipping of a single ladderene. (**B**) Force-modified potential energy surface showing consecutive ring openings of the cyclobutane units in the ladderene to give an oligoene. (**C**) Force-extension curve simulated using molecular dynamics.

copolymers with insoluble PA in the middle and soluble unactivated polyladderene at the ends (Fig. 3A). PA-containing block copolymers are difficult to synthesize (*26*–*28*), especially in all-trans configuration. The *trans*-PA copolymers were expected to self-assemble into unique nanostructures driven by the aggregation of the long PA block and stabilization of the unactivated polyladderene block. Indeed, dynamic light scattering (DLS) of the sonicated solutions showed the formation of micelles with a hydrodynamic radius growing from 115 to 500 nm, as sonication time increased from 20 s to 20 min (fig. S6). Transmission electron microscopy (TEM) of these samples revealed evolution of nanostructures (Fig. 3F) in this time frame from spherical micelles to elongated and interconnected wormlike structures. After 2 hours of sonication, meshes of interconnected nanowires were clearly observed. These nanowires were presumably composed of an aggregated PA core encapsulated by a solubilizing polyladderene corona. To measure the electrical conductivity of these encapsulated PA nanowires, we drop-cast the solution of activated sample onto a microelectrode array to form a film by simple solvent evaporation without doping or annealing or alignment (fig. S7). We measured a conductivity of 2.6×10^{-7} S/cm, which is about two orders of magnitude lower than the reported value for Shirakawa's surface-grown aligned *trans*-PA film sample (*24*). This relatively low conductivity is still a compelling initial result, considering the encapsulation by an insulating corona and the meshed, rather than bulk, nanowire structures. The measured conductivity further supported the formation of an interconnected network of semiconducting PA domains.

To gain more insight into the facile mechanochemistry of polyladderene, we first computed the force-modified potential energy surface (FMPES) for the unzipping of a single ladderene under different pulling forces (Fig. 4, A and B). Calculations were performed on model ladderene **13**; attachment points (atoms where the force is exerted) were chosen as the carbon atoms farthest from the ladderane core. For a series of external forces ranging from 0 to 3 nN, minimum energy pathways were optimized using the nudged elastic band (NEB) method (*34*), which yields reaction coordinates and energy profiles. Electronic structure calculations were performed with graphics processing unit (GPU)–accelerated complete active space self-consistent field (CASSCF) theory (*35*) with 6-31 g* basis. The CASSCF method is advantageous in this case because it can accurately describe a multireference character in the electronic wave function, which is critical for potential radical intermediates. We found a single barrier for each of the two sequential cyclobutane unzipping events, which involve simultaneous breaking of two σ bonds and formation of two π bonds (these are the four electrons and orbitals in the active space). The structure with two opened rungs (**15**) is a metastable intermediate, whereas the structures with 1 or 3 opened rungs (**14** and **16**, respectively) are transient transition states. Inspection of the electronic wave function confirmed that transition-state structures are diradicals with a strong multireference character (table S1). According to Fig. 4B, two consecutive large barriers have to be surmounted for the unzipping event to take place in the absence of pulling force. Application of force lowers these barriers; the second barrier remains slightly lower than the first at all force levels (fig. S20), and both become negligible at 3.0 nN force, at which point the unzipping process becomes spontaneous.

We further calculated the force-extension curve for one ladderene unit on the FMPES at UB3LYP/6-31 g* level of theory (Fig. 4C). Comparison with CASSCF was used to validate the choice of exchange-correlation functional and to ensure density functional theory convergence to the diradical solution (fig. S21). Constant temperature ab initio steered molecular dynamics (*36*) at 279 K was performed for 10 ps at each of a variety of external forces ranging from 0 to 4.5 nN. For each external force, the contour length corresponding to one monomer was recorded at the end of the simulation by taking the average of distances over the last 0.5 ps of the simulation. Equilibrium analysis at 0 K was also performed to corroborate the molecular dynamics analysis (fig. S23). The force-extension curve has a single plateau at 3.1 nN force with the monomer extending by 10 Å or twice the contour length at unzipping of the entire ladderene (Fig. 4C), and the intermediate **15** was not observed. This all-or-none unzipping behavior is consistent with the reaction barrier analysis and suggests that ladderene is a privileged design motif for generating oligoenes with continuous extended conjugation.

We envision the emergence of additional force-responsive polymers that undergo mechanically triggered macromolecular structural reconfiguration and drastically change their intrinsic properties, thereby converting mechanical stimuli into a diverse array of functions.

REFERENCES AND NOTES

1. C. R. Hickenboth *et al.*, *Nature* **446**, 423–427 (2007).
2. J. M. Lenhardt *et al.*, *Science* **329**, 1057–1060 (2010).
3. J. Li, C. Nagamani, J. S. Moore, *Acc. Chem. Res.* **48**, 2181–2190 (2015).
4. M. Chalfie, *Nat. Rev. Mol. Cell Biol.* **10**, 44–52 (2009).
5. D. A. Davis *et al.*, *Nature* **459**, 68–72 (2009).
6. Y. Chen *et al.*, *Nat. Chem.* **4**, 559–562 (2012).
7. E. Ducrot, Y. Chen, M. Bulters, R. P. Sijbesma, C. Creton, *Science* **344**, 186–189 (2014).
8. A. L. Ramirez *et al.*, *Nat. Chem.* **5**, 757–761 (2013).
9. C. E. Diesendruck *et al.*, *Nat. Chem.* **6**, 623–628 (2014).
10. M. B. Larsen, A. J. Boydston, *J. Am. Chem. Soc.* **135**, 8189–8192 (2013).
11. C. E. Diesendruck *et al.*, *J. Am. Chem. Soc.* **134**, 12446–12449 (2012).
12. A. Piermattei, S. Karthikeyan, R. P. Sijbesma, *Nat. Chem.* **1**, 133–137 (2009).
13. T. A. Skotheim, J. Reynolds, *Conjugated Polymers: Theory, Synthesis, Properties, and Characterization* (CRC Press, 2006).
14. Q. Z. Yang *et al.*, *Nat. Nanotechnol.* **4**, 302–306 (2009).
15. M. J. Kryger *et al.*, *J. Am. Chem. Soc.* **132**, 4558–4559 (2010).
16. M. J. Kryger, A. M. Munaretto, J. S. Moore, *J. Am. Chem. Soc.* **133**, 18992–18998 (2011).
17. Z. S. Kean, A. L. Black Ramirez, Y. Yan, S. L. Craig, *J. Am. Chem. Soc.* **134**, 12939–12942 (2012).
18. Z. S. Kean, Z. Niu, G. B. Hewage, A. L. Rheingold, S. L. Craig, *J. Am. Chem. Soc.* **135**, 13598–13604 (2013).
19. J. I. Brauman, W. C. Archie Jr., *Tetrahedron* **27**, 1275–1280 (1971).
20. K. Rudolf, D. C. Spellmeyer, K. N. Houk, *J. Org. Chem.* **52**, 3708–3710 (1987).
21. J. S. Sinninghe Damsté *et al.*, *Nature* **419**, 708–712 (2002).
22. J. A. M. Mercer *et al.*, *J. Am. Chem. Soc.* **138**, 15845–15848 (2016).
23. R. H. Grubbs, E. Khosravi, *Handbook of Metathesis, Volume 3: Polymer Synthesis, 2nd Ed.* (Wiley-VCH, 2015).
24. H. Shirakawa, E. J. Louis, A. G. MacDiarmid, C. K. Chiang, A. J. Heeger, *J. Chem. Soc. Chem. Commun.* **16**, 578–580 (1977).
25. W. Liu, J. T. Groves, *J. Am. Chem. Soc.* **132**, 12847–12849 (2010).
26. G. L. Baker, F. S. Bates, *Macromolecules* **17**, 2619–2626 (1984).
27. O. A. Scherman, I. M. Rutenberg, R. H. Grubbs, *J. Am. Chem. Soc.* **125**, 8515–8522 (2003).
28. K.-Y. Yoon *et al.*, *J. Am. Chem. Soc.* **134**, 14291–14294 (2012).
29. C. B. Gorman, E. J. Ginsburg, R. H. Grubbs, *J. Am. Chem. Soc.* **115**, 1397–1409 (1993).
30. H. W. Gibson, S. Kaplan, R. A. Mosher, W. M. Prest, R. J. Weagley, *J. Am. Chem. Soc.* **108**, 6843–6851 (1986).
31. I. Harada, M. Tasumi, H. Shirakawa, S. Ikeda, *Chem. Lett.* **7**, 1411–1414 (1978).
32. F. B. Schügerl, H. Kuzmany, *J. Chem. Phys.* **74**, 953–958 (1981).
33. T. Q. Nguyen, H.-H. Kausch, in *Macromolecules: Synthesis, Order and Advanced Properties* (Springer, Berlin, Heidelberg, 1992), pp. 73–182.
34. M. U. Bohner, J. Meisner, J. Kästner, *J. Chem. Theory Comput.* **9**, 3498–3504 (2013).
35. E. G. Hohenstein, N. Luehr, I. S. Ufimtsev, T. J. Martínez, *J. Chem. Phys.* **142**, 224103 (2015).
36. M. T. Ong, J. Leiding, H. Tao, A. M. Virshup, T. J. Martínez, *J. Am. Chem. Soc.* **131**, 6377–6379 (2009).

ACKNOWLEDGMENTS

This work was supported by the U.S. Army Research Office under grant number W911NF-15-1-0525 and Stanford University. J.A.M.M. thanks the National Science Foundation for a graduate fellowship. R.P. acknowledges support from Marie Curie Cofund, Beatriu de Pinós fellowship (AGAUR 2014 BP-A 00094). T.J.M. acknowledges support from Office of Naval Research grant N00014-12-1-0828 and the Global Climate and Energy Project. This work used the XStream computational resource supported by the National Science Foundation Major Research Instrumentation program (ACI-1429830). L.C. acknowledges support from the National Science Foundation CAREER Award 1453247. We thank J. I. Brauman for helpful discussion, Z. Bao for conductivity measurement, A. F. Marshall at Stanford Nano Shared Facilities for helping with TEM imaging, and Materia Inc. for a gift of Grubbs catalyst. All data are available in the supplementary materials. The authors declare no competing financial interest.

SUPPLEMENTARY MATERIALS

www.sciencemag.org/content/357/6350/475/suppl/DC1
Materials and Methods
Supplementary Text
Figs. S1 to S23
Tables S1 to S6
Movies S1 and S2
References (*37*–*46*)

23 March 2017; accepted 15 June 2017
10.1126/science.aan2797

Mechanochemical unzipping of insulating polyladderene to semiconducting polyacetylene

Zhixing Chen, Jaron A. M. Mercer, Xiaolei Zhu, Joseph A. H. Romaniuk, Raphael Pfattner, Lynette Cegelski, Todd J. Martinez, Noah Z. Burns and Yan Xia

Science **357** (6350), 475-479.
DOI: 10.1126/science.aan2797

Forcing polymers to be semiconductors

In mechanochemistry, the application of force to a polymer is used to pry open specific chemical bonds. Chen *et al.* leveraged this technique to produce semiconducting blocks of polyacetylene in an insulating precursor. Ring-opening metathesis polymerization tethered together a series of fused four-carbon rings, reminiscent of the unusual ladderane membrane lipids of anaerobic ammonium-oxidizing bacteria. Subsequently, sonication unzipped these strained rings into alternating C=C double bonds, thereby extending π-conjugation along the polymer backbone.

Science, this issue p. 475